Compositional segregation and solid solution in the lead-dominant alunite-type minerals from Broken Hill, N.S.W.

K. J. RATTRAY, M. R. TAYLOR, D. J. M. BEVAN

Department of Chemistry , Flinders University, GPO Box 2100 Adelaide, South Australia 5000, Australia.

AND

A. PRING

Department of Mineralogy, South Australian Museum, North Terrace, Adelaide, South Australia 5000, Australia

Abstract

A study of the composition and unit cell data of a suite of lead-rich minerals of the alunite–jarosite group from the oxidized zone of the ore body at Broken Hill, New South Wales, Australia, has revealed almost complete XO_4 (X = As, P, S) solid solution in these minerals at this deposit. The species in the group noted are hidalgoite, hinsdalite, beudantite, segnitite and plumbogummite. These minerals at Broken Hill exhibit a number of growth textures, including oscillatory zoning, colloform banding and replacements. Zoning in these minerals is due to the segregation of Al- and Fe-rich members, and compositions indicate a strong coupling of Fe^{3+} with AsO_4^{3-} and Al with PO_4^{3-}.

KEYWORDS: segregation, solid-solution, hidalgoite, plumbogummite, alunite-type minerals, Broken Hill, Australia.

Introduction

SOME forty minerals have the alunite-jarosite structure-type. They have the general formula, $AB_3(XO_4)_2(OH)_6$, where A represents a large cation such as K^+, Na^+, Ca^{2+} or Pb^{2+}, B represents Fe^{3+} or Al^{3+} in octahedral coordination, and (XO_4) represents a tetrahedral anion such as SO_4^{2-}, PO_4^{3-}, AsO_4^{3-} or SiO_4^{4-}, and protonated groups, like $(PO_3OH)^{2-}$ (Blount, 1974; Botinelly, 1976; Scott, 1987). In addition to the pure phosphate, sulphate and arsenate end-members, such as plumbogummite ($PbAl_3H(PO_4)_2(OH)_6$), a number of mid-member compositions are defined as distinct species; for example hidalgoite ($PbAl_3(AsO_4)(SO_4)(OH)_6$). The Pb-dominant alunite–jarosite minerals $PbB_3(XO_4)_2(OH)_6$, where X = P, S, or As, have been classified into six groups (Scott, 1987): the beudantite, hinsdalite, plumbogummite, alunite, jarosite and lusungite groups. The nomenclature of the lusungite group has recently been revised following the discreditation of lusungite and the description of two new end-members (Birch *et al.*, 1992; Pring *et al.*, 1995); the group is now designated as the segnitite group. Current nomenclature and chemical relationships among the various groups are summarized in Table 1. This paper reports further studies on minerals in these groups.

Accurate crystal structure determinations have been reported for a number of the end-member and mid-member minerals. The anions in beudantite $PbFe_3(AsO_4)(SO_4)(OH)_6$, were found to be disordered on a single crystallographic site (Szymanski, 1988; Giuseppetti and Tadini, 1989), whereas in corkite, $PbFe_3(PO_4)(SO_4)(OH)_6$, the PO_4^{3-} and SO_4^{2-} groups are ordered onto two distinct sites, resulting in a change in symmetry from $R\bar{3}m$ to $R3m$ (Giuseppetti and Tadini, 1987). The nature of order–disorder relationships for the XO_4 anions in these minerals is a question yet to be fully resolved. Closely allied with this problem is to what extent solid solution occurs. Numerous workers have reported deviations in the

Mineralogical Magazine, October 1996, Vol. 60, pp. 779–785

TABLE 1. Nomenclature and chemical relationships among the alunite-jarosite groups investigated

Mineral Groups	Composition	a_0 (Å)	c_0 (Å)	Vol Å^3	Reference
Alunite group	$AAl_3(XO_4)_2(OH)_6$				
Jarosite group	$AFe_3(XO_4)_2(OH)_6$				
Plumbojarosite	$PbFe_6(SO_4)_4(OH)_{12}$	7.315	33.788	1565.7	PDF
Beudantite group	$AFe_3(XO_4)_2(OH)_6$				
Beudantite	$PbFe_3(AsO_4,SO_4)_2(OH)_6$*	7.32	17.02	789.7	PDF
Corkite	$PbFe_3(PO_4)(SO_4)(OH)_6$	7.22	16.66	752.1	PDF
Hinsdalite group	$AAl_3(XO_4)_2(OH)_6$*				
Hinsdalite	$PbAl_3(PO_4,SO_4)_2(OH)_6$*	6.99	16.8	710.8	PDF
Hidalgoite	$PbAl_3(AsO_4,SO_4)_2(OH)_6$*	7.04	16.99	729.2	PDF
Segnitite group	$AFe_3H(XO_4)_2(OH)_6$				
Segnitite	$PbFe_3H(AsO_4)_2(OH)_6$	7.359	17.113	802.5	Birch *et al.* (1992)
Kintoreite	$PbFe_3H(PO_4)_2(OH)_6$	7.325	16.900	785.3	Pring *et al.* (1995)
Plumbogummite group	$AAl_3H(XO_4)_2(OH)_6$				
Plumbogummite	$PbAl_3H(PO_4)_2(OH)_6$	7.017	16.75	714.2	PDF
Philpsbornite	$PbAl_3H(AsO_4)_2(OH)_6$	7.11	17.05	746.4	Walenta *et al.* (1982)

* ratio of anions on the XO_4 site variable, either anion maybe dominant.

ideal 1:1 ratio of anions in the mid-member compositions (Palache *et al.*, 1951; Smith *et al.*, 1953; Birch *et al.*, 1992). In beudantite, hidalgoite and corkite, excess SO_4^{2-} has been reported, and some apparent substitution of AsO_4^{3-} by PO_4^{3-} has also been noted in beudantite. Hinsdalite, with PO_4^{3-} in excess over SO_4^{2-}, has been reported from a number of localities (Palache *et al.*, 1951; Wambeke, 1971), and extensive compositional fields have also been reported between kintoreite and segnitite (Birch *et al.*, 1992; Pring *et al.*, 1995). Such results suggest that extended compositional fields occur, at least at some deposits, and that there must be a degree of disorder on the XO_4 sites. On the other hand, sharp chemical zoning, which has been observed in samples consisting of intergrowths of beudantite and plumbojarosite (Simpson, 1938), and plumbogummite, hinsdalite and hidalgoite (Fortsch, 1967), suggests ordering of XO_4 anions and therefore limited solid solution.

To further explore the nature of compositional fields in these minerals, we have investigated the variation in composition for a suite of relatively abundant alunite-group minerals from the oxidized zone of the ore body at Broken Hill, New South Wales, Australia.

Experimental

Specimens examined in this study come from the Kintore, Blackwoods and Block 14 opencuts, Broken Hill, New South Wales. A description of the geology and mineralogy of this portion of the Broken Hill deposit has been given by Birch (1990) and Birch and van der Heyden (1988). The initial aim of this study was to carry out single-crystal structural analyses of these minerals but no suitable crystals of the Al-dominant minerals could be found: hinsdalite, hidalgoite and plumbogummite occur only as masses, microcrystalline crusts or as pseudomorphs after pyromorphite or mimetite.

Powder X-ray diffraction patterns were recorded using an 80 mm, Hägg-Guinier camera with monochromated Cu-$K\alpha_1$ (λ = 1.54051 Å) radiation, with elemental Si as an internal standard. Preliminary identification was made by referring to the JCPDS powder diffraction file. Subsequently, the patterns were fully indexed and unit cell parameters of the minerals refined by least squares methods.

Considerable care was taken to ensure that as far as possible chemical and X-ray powder data were obtained on the same fragments from the various specimens. In most cases, fragments were split in two; one part was crushed for X-ray work and the other mounted and polished for microanalysis. Chemical analyses were performed using a CAMECA SX51 electron probe microanalyser with a wavelength-dispersion analysis system, operating under the following conditions: 15 kV accelerating voltage, 20 nA beam current, counting time 10 s on the peak, 5 s for the background. Initial analyses were obtained using Pb metal as the lead standard; however, a synthetic PbS standard was found to give slightly better analyses. The standards for the

other elements were Al metal (Al), galena (S), hematite (Fe), fluorapatite (P), arsenopyrite (As), wollastonite (Si), sphalerite (Zn), and Cu metal (Cu).

Results and discussion

Unit cell dimensions were refined for all alunite-type minerals present in quantities sufficient to enable an unambiguous assignment of indices. In general the unit cell parameters are close to those reported in the literature for the various minerals. The chemical analyses determined for each sample correlate well with the powder X-ray diffraction data, and in several instances enabled the clarification of X-ray results, particularly in the positive identification of plumbogummite and hinsdalite where the unit cell parameters are very similar (see Table 1). Chemical data and unit cell parameters for the various specimens are summarized in Table 2. The analyses are calculated on the basis of two XO_4 anions and, in general, are in good agreement with the structural formulae. Some analyses, however, show an excess of lead on the *A* cation site. This seems to be a common problem in the electron probe microanalyses of these minerals, as it has previously been reported by a number of other workers (e.g. Scott 1987; Birch and van der Heyden 1988), and it is most likely associated with the choice of the lead standard. Unsuccessful attempts were made in this study to prepare a more suitable lead standard, either a lead arsenate or phosphate. The possibility that the excess on the *A* site is due to the presence of some unanalysed components on the XO_4 sites, such as CO_3^{2-} or VO_4^{3-} can be ruled out as a significant factor as it would result in an excess of cations on the *B* site, which was not observed here.

Five of the specimens were found to be composed of a single alunite-group mineral (Nos. 1–5), whereas the four others are intergrowths of several alunite–jarosite minerals (Nos. 6–9) (Table 2). A range of compositions was found, with many exhibiting significant substitution on the XO_4 site away from end-member or mid-member compositions (Fig. 1).

Three distinct intergrowth textures were observed: oscillatory zoned 'single crystals', colloform banding and replacement textures (Fig. 2). In some instances the fine scale of the compositional segregation prevented the acquisition of reliable chemical analyses for the individual minerals. In general, chemical data are included here only if the minerals occur in suitably large domains (> 3 μm in diameter), but even with this qualification some contribution from the matrix cannot be ruled out in some analyses. It is clear that the zoning in these minerals is due to the segregation of Al- and Fe-rich members, and also reveals a strong coupling of AsO_4^{3-} with Fe^{3+} and PO_4^{3-} with Al^{3+}.

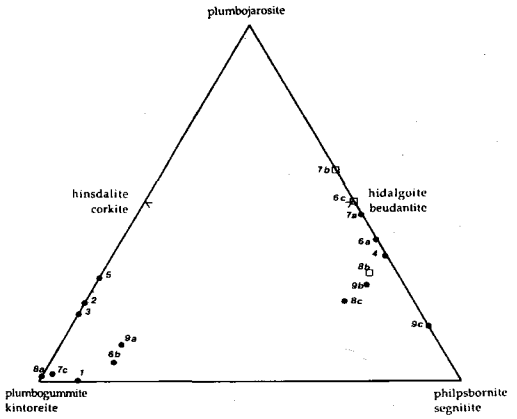

FIG. 1. Compositional diagram showing the compositions of the Broken Hill specimens in relationship to the end- and mid-members. The specimen numbering refers to Table 2. Filled circles represent Al-dominant compositions and open squares represent Fe-dominant compositions.

As noted in the introduction, atomic substitutions can occur in nature on the *A*, *B* and XO_4 sites in these alunite-like minerals. In the suite of Pb-rich alunite-like minerals examined in this work no substitution was observed on the *A* site. All compositions are pure Pb end-members. The limit of Fe^{3+} substitution in Al-rich members was found to be 5% (No. 2), and the extent of Al substitution in Fe-rich members is up to 22% (segnitite No. 9). The replacement of Al^{3+} by Fe^{3+} appears to be more restricted than the reverse, but this may be due to the very fine-grained nature of the Fe-rich regions within an Al-dominant host. These domains commonly are only several micrometres across, and as previously noted some contribution from the matrix cannot be ruled out. Minor substitution, in general <2%, of Cu^{2+} and Zn^{2+} was also noted in some analyses. These results are consistent with previous studies on alunite-jarosite minerals from the oxidized zone of the Broken Hill deposit (Birch *et al.*, 1992). More extensive Al-Fe solid solution was reported for alunite-type minerals from the Mount Isa region, northwest Queensland (Scott, 1987). He found that complete Fe-Al solid solution was coupled with occupancy of the *A* site by divalent cations. For compositions with less than 80% A^{2+} on the *A* site, Scott reported a miscibility gap in the series. Although there are some problems with contamination by hematite in many of Scott's (1987) more fine-grained specimens, and it is unclear whether evidence of fine-scale zoning was sought, it seems likely that there are major differences between the two occurrences. Complete solid solution

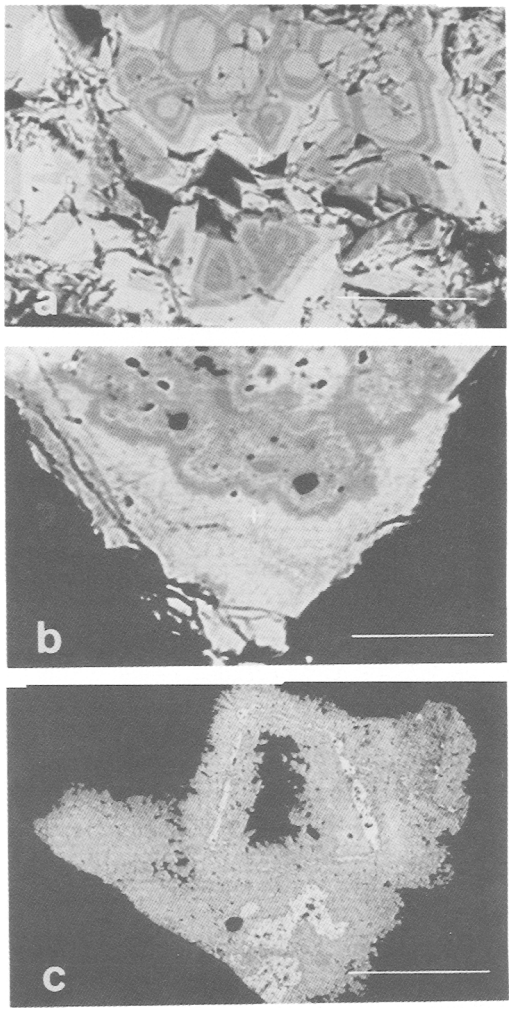

FIG. 2. Backscattered electron images illustrate growth textures in the alunite–jarosite minerals from Broken Hill. (*a*) Oscillatory zoning in single crystals (Specimen No. 9); the light phase is segnitite, the medium-contrast phase is hidalgoite, and the dark phase is plumbogummite. The scale bar is 20 μm in length. (*b*) Colloform banding in specimen No. 8. The light phase is beudantite, the medium-contrast phase is hidalgoite, and the dark phase is plumbogummite. The scale bar is 20 μm in length. (*c*) Replacement texture in specimen No. 6. The light phase at the core of the crystal is beudantite, and the darker fibrous crystals are hidalgoite and plumbogummite. The scale bar is 200 μm in length.

between synthetic alunite and jarosite has been demonstrated by Brophy *et al.* (1962), but no studies of solid solution have been reported for synthesized members of the mineral groups under discussion here.

Extensive substitutions occur on the XO_4 site in the Broken Hill suite; however, the nature of these substitutions is more complex (Table 2). Five monomineralic samples have only two components in the XO_4 sites. Of the three plumbogummites analysed (Nos. 1 to 3), two contain some SO_4^{2-} but neglibible AsO_4^{3-}; while the third specimen contains some AsO_4^{3-}, but no SO_4^{2-}. All three show significant deviation from the end-member composition, as do the hidalgoite and hinsdalite specimens (Nos. 4 and 5) from the ideal mid-member composition (Fig. 1). In each of the four multiphase samples (Nos. 6–9), three distinct compositions were identified; in general, the multiphase samples show significant variation from the ideal end-member and mid-member compositions, and many have three components in the XO_4 sites.

Figure 3 illustrates the effect that substitutions on the XO_4 and B sites have on the cell volumes. The substitution of Fe on the B site has the largest effect on the cell volume: that of the pure Fe end-member is around 7.5% greater than that for the equivalent Al composition. The substitution of AsO_4^{3-} also increases the cell volume but the expansion in this case is between 2 and 4% over the PO_4^{3-} and SO_4^{2-} end-members. There is little effect on cell volume when PO_4^{3-} replaces SO_4^{2-} ions. The composition *vs.* cell volume plots shown in Fig. 3 show there is good correlation between the compositional data and cell data for the alunite–jarosite minerals examined in this study. The cell volumes of intermediate compositions all lie, within error limits, on the linear trend between end-members. There is no deviation from this trend about the mid-member compositions, which might indicate ordering on the anion sites.

The co-crystallization of beudantite and segnitite in plumbogummite and hidalgoite indicates strong chemical coupling of Fe and AsO_4^{3-} in these minerals. The formulae show considerable deviation from the ideal end- and mid-member compositions, indicating that there is probably no ordering on the XO_4 anion site. This study and those of Palache *et al.* (1951), Smith *et al.* (1953), Birch *et al.* (1992), Wambeke (1971), Scott (1987) and Pring *et al.* (1995) show that there is considerable, almost continuous, XO_4 solid solution in the alunite–jarosite minerals and that the status of the mid-member compositions as distinct minerals must be considered as doubtful.

Acknowledgements

Thanks to Huw Rosser at CEMMSA, University of Adelaide, for his valuable assistance with the probe

TABLE 2. Chemical composition and unit cell dimensions for alunite-jarosite minerals from the Kintore, Block 14 and Blackwoods Opencut pits, Broken Hill, New South Wales

No.	Mineral	Composition	a_o (Å)	c_o (Å)	Vol (Å3)
(1)	plumbogummite	$Pb_{1.17}Al_{3.03}[(P_{0.9}As_{0.1})O_4]_2(OH,H_2O)_6$	7.0192(9)	16.739(3)	714.2(2)
(2)	plumbogummite	$Pb_{1.24}(Al_{2.85}Fe_{0.16})[(P_{0.77}S_{0.23})O_4]_2(OH,H_2O)_6$	7.0251(6)	16.776(2)	717.0(1)
(3)	plumbogummite	$Pb_{1.17}Al_{2.91}[(P_{0.81}S_{0.19})O_4]_2(OH, H_2O)_6$	7.0134(6)	16.760(3)	713.9(2)
(4)	hidalgoite	$Pb_{1.21}(Al_{2.99}Fe_{0.01})[(As_{0.65}S_{0.35})O_4]_2(OH,H_2O)_6$	7.076(2)	16.995(6)	737.0(4)
(5)	hinsdalite	$Pb_{1.25}(Al_{3.00}Fe_{0.01})[(P_{0.72}S_{0.28})O_4]_2(OH,H_2O)_6$	7.0107(7)	16.778(3)	714.1(2)
(6) a	hidalgoite	$Pb_{1.06}(Al_{2.94}Fe_{0.08}Cu_{0.05}Zn_{0.04})[(As_{0.61}S_{0.39})O_4]_2(OH,H_2O)_6$	7.067(1)	16.987(4)	734.9(2)
b	plumbogummite	$Pb_{1.03}(Al_{2.86}Fe_{0.13}Zn_{0.08}Cu_{0.02})[(P_{0.80}S_{0.15}As_{0.05})O_4]_2(OH,H_2O)_6$	7.003(3)	16.76(2)	711.7(6)
c	beudantite	$Pb_{1.20}(Fe_{2.90}Al_{0.21}Cu_{0.04}Zn_{0.01})[(As_{0.50}S_{0.48}Si_{0.02})O_4]_2(OH,H_2O)_6$	7.345(7)	17.06(2)	796(2)
(7) a	hidalgoite	$Pb_{1.00}(Al_{2.95}Cu_{0.16}Fe_{0.03})[(As_{0.53}S_{0.45}Si_{0.02})O_4]_2(OH,H_2O)_6$	7.0667(7)	16.989(2)	734.8(2)
b	beudanite	$Pb_{0.95}(Fe_{2.60}Al_{0.20}Cu_{0.06}Zn_{0.02})[(S_{0.57}As_{0.43})O_4]_2(OH,H_2O)_6$	–	–	–
c	plumbogummite	$Pb_{0.85}(Al_{2.74}Fe_{0.09}Cu_{0.02}Zn_{0.02})[(P_{0.96}S_{0.03}As_{0.01})O_4]_2(OH,H_2O)_6$	–	–	–
(8) a	plumbogummite	$Pb_{0.99}(Al_{2.95}Fe_{0.09}Cu_{0.07}Zn_{0.02})[(P_{0.97}Si_{0.02}S_{0.01})O_4]_2(OH,H_2O)_6$	7.027(2)	16.778(4)	717.5(3)
b	beudantite	$Pb_{1.03}(Fe_{2.47}Al_{0.37}Cu_{0.14}Zn_{0.04})[(As_{0.63}S_{0.30}P_{0.07})O_4]_2(OH,H_2O)_6$	7.315(5)	17.07(2)	791(2)
c	hidalgoite	$Pb_{1.02}(Al_{2.52}Fe_{0.36}Cu_{0.06})[(As_{0.62}S_{0.22}P_{0.16})O_4]_2(OH,H_2O)_6$	–	–	–
(9) a	plumbogummite	$Pb_{1.02}(Al_{2.86}Fe_{0.07}Cu_{0.04}Zn_{0.02})[(P_{0.76}S_{0.15}As_{0.09})O_4]_2(OH,H_2O)_6$	7.022(2)	16.797(4)	171.3(3)
b	hidalgoite	$Pb_{1.06}(Al_{2.98}Fe_{0.12}Cu_{0.13}Zn_{0.04})[(As_{0.64}S_{0.28}P_{0.08})O_4]_2(OH,H_2O)_6$	7.076(7)	17.06(1)	739.9(6)
c	segnitite	$Pb_{1.04}(Fe_{2.08}Al_{0.66}Cu_{0.05}Zn_{0.04})[(As_{0.92}S_{0.08})O_4]_2(OH,H_2O)_6$	7.335(5)	17.11(2)	797(1)

* The South Australian Museum catalogue numbers for the specimens are:
(1) G 13161, (2) G17074, (3) G17555, (4) G13254, (5) G15427, (6) G13253, (7) G14348, (8) G15634, (9) G18217

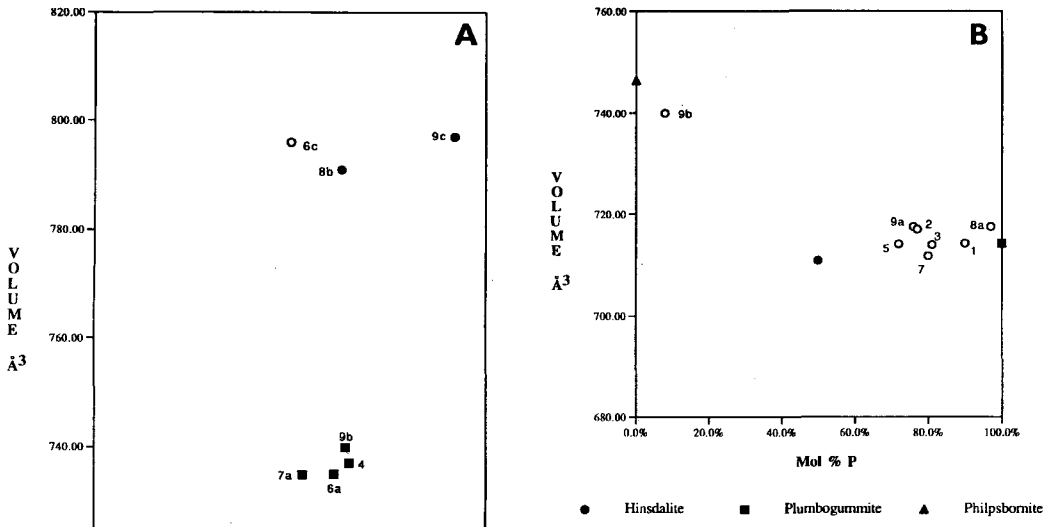

FIG. 3. The relationship between volume and anion composition in the Pb-dominant end-members of the alunite–jarosite minerals. (*a*) Cell volume *vs.* mole fraction of As on the XO_4 site. Al-dominant compositions are represented by squares, Fe-dominant by circles. (*b*) Cell volume *vs.* mole fraction of P on XO_4 site for Al-rich compositions.

analyses. The constructive comments of the anonymous referees are also gratefully acknowledged.

References

Birch, W.D. (1990) Minerals from Kintore and Block 14 opencuts, Broken Hill, N.S.W.; review of recent discoveries, including tsumebite, kipushite and otavite. *Austral. Mineral.*, **5**, 125–41.

Birch, W.D. and van der Heyden, A. (1988) Minerals from the Kintore Opencut, Broken Hill, New South Wales. *Mineral. Record*, **19**, 425–36.

Birch, W. D., Pring, A. and Gatehouse, B. M. (1992) Segnitite, $PbFe_3H(AsO_4)_2(OH)_6$, a new mineral in the lusungite group from Broken Hill, New South Wales, Australia. *Amer. Mineral.*, **77**, 656–59.

Blount, A. M. (1974) The crystal structure of crandallite. *Amer. Mineral.* , **59**, 41–7.

Botinelly, T. (1976) A review of the minerals of the alunite-jarosite, beudantite and plumbogummite groups *J. Res. U.S Geol. Survey*, **4**, 213–6.

Brophy, G. P., Scott, E. S. and Snellgrove, R. A. (1962) Sulfate studies 2. Solid solution between alunite and jarosite. *Amer. Mineral.*, **47**, 112–26.

Fortsch, E. B. (1967)'Plumbogummite' from Roughten Gill, Cumberland. *Mineral. Mag.*, **36** 530–8.

Giuseppetti, G. and Tadini, C. (1987) Corkite $PbFe_3(SO_4)(PO_4)(OH)_6$, its crystal structure and ordered arrangement of tetrahedral cations. *Neues Jahrb. Mineral. Mh.*, 71–81.

Giuseppetti, G. and Tadini, C. (1989) Beudantite $PbFe_3(SO_4)(AsO_4)(OH)_6$, its crystal structure, tetrahedral site disordering and scattered Pb distribution. *Neues Jahrb. Mineral. Mh.*, 27–33.

Palache, C., Berman, H. and Frondel, C. (1951) *Dana's system of mineralogy*, John Wiley and Sons, New York, **2**, 912–4.

Pring, A., Birch, W.D., Dawe, J.R., Taylor, M.R., Deliens, M. and Walenta, K. (1995) Kintoreite, $PbFe_3(PO_4)_2(OH,H_2O)_6$, a new mineral of the jarosite-alunite family, and lusungite discredited. *Mineral. Mag.*, **59**, 143–8.

Scott, K. M. (1987) Solid solution in, and classification of, gossan derived members of the alunite-jarosite family, northwest Queensland, Australia. *Amer. Mineral.*, **72**, 178–87.

Simpson, E.S. (1938) Beaudantite-plumbojarosite mixture. Contributions to the mineralogy of Western Australia *J. Roy. Soc. W.A.* **24**, 110–2.

Smith, R.L., Simons, F.S. and Vlisidis, A.C. (1953) Hidalgoite, a new mineral. *Amer. Mineral.*, **38**, 1218–24.

Szymanski, J.T. (1988) The crystal structure of beudantite $Pb(Fe,Al)_3[(As,S)O_4]_2(OH)_6$. *Can.*

Mineral., **26**, 923–32.

Walenta, K., Zwiener, M. and Dunn, P. J. (1982) Philipsbornite, a new mineral of the crandallite series from Dundas, Tasmania. *Neues Jahrb. Mineral. Mh.*, 1–5.

Wambeke, L. van (1971) Hinsdalite and corkite: Indicator minerals in Central Africa. *Mineral. Deposita*, **6**, 130–2.

[*Manuscript received 27 November 1995: revised 8 February 1996*]